Cell

Selective Protein Synthesis by Ribosomes with a Drug-Obstructed Exit Tunnel

Krishna Kannan,[1] Nora Vázquez-Laslop,[1] and Alexander S. Mankin[1,*]
[1]Center for Pharmaceutical Biotechnology, University of Illinois at Chicago, 900 S. Ashland Avenue, Chicago, IL 60607, USA
*Correspondence: shura@uic.edu
http://dx.doi.org/10.1016/j.cell.2012.09.018

SUMMARY

The polypeptide exit tunnel is an important functional compartment of the ribosome where the newly synthesized proteins are surveyed. The tunnel is the target of clinically important macrolide antibiotics. Macrolides plug the tunnel and are believed to stop production of all proteins. Contrary to this view, we show that drug-bound ribosomes can synthesize a distinct subset of cellular polypeptides. The structure of a protein defines its ability to thread through the antibiotic-obstructed tunnel. Synthesis of certain polypeptides that initially bypass translational arrest can be stopped at later stages of elongation while translation of some proteins goes to completion. Our findings reveal that small-molecule effectors can accentuate the discriminatory properties of the ribosomal exit tunnel and that macrolide antibiotics reshape the cellular proteome rather than block global protein synthesis.

INTRODUCTION

The proteins assembled in the peptidyl transferase center (PTC) of the ribosome leave through the nascent peptide exit tunnel (NPET). The ~100 Å long and 10–20 Å wide NPET starts at the PTC and penetrates through the body of the large ribosomal subunit (Yonath et al., 1987; Frank et al., 1995; Nissen et al., 2000; Voss et al., 2006) (Figure 1A). It ensures the successful passage of newly made proteins out of the ribosome, and thus is able to accommodate a vast variety of nascent peptide sequences. The tunnel, however, is not an impartial conduit. Some nascent peptides can specifically interact with the NPET, altering the rate of translation elongation and, in extreme cases, leading to translation arrest. The peptide monitoring and discriminating properties of the NPET are used by the cell for optimizing the regulation of gene expression, protein targeting, and folding (reviewed in Ito et al., 2010). The recognition of the individual nascent peptide in the NPET and the ribosomal response can be sensitive to cellular cues, such as the concentration of specific small metabolites. For example, nascent peptide-mediated translation arrest at the *tnaC* gene is stimulated by tryptophan (Gong and Yanofsky, 2002); the concentration of arginine regulates elongation of the arginine attenuator peptides in fungi (Fang et al., 2004), while ribosome progression along the cystathionine γ-synthase gene in *Arabidopsis* is sensitive to the concentration of S-adenosyl-methionine (Onouchi et al., 2005). In none of these cases is it understood how the small molecules modulate the progression of the nascent peptide through the NPET, because their binding sites remain a mystery.

The ribosomal NPET is the site of action of clinically important macrolide antibiotics (Vázquez, 1966) (Figure 1B). The prototype of this class, erythromycin (ERY), shows strong bacteriostatic activity against a broad range of Gram-positive and some Gram-negative pathogens (Oleinick, 1975). The macrolides of the second generation (e.g., azithromycin) exhibit improved chemical stability and a superior spectrum of coverage. The newest generation of macrolides, known as ketolides (e.g., telithromycin [TEL]; Figure 1B), is even more potent: they inhibit bacteria at lower drug concentrations and, in addition, exhibit increased bactericidal activity against some pathogens (Ackermann and Rodloff, 2003; Hamilton-Miller and Shah, 1998).

Treatment of sensitive bacteria with macrolides curtails protein synthesis and leads to the accumulation of peptidyl-transfer RNAs (peptidyl-tRNAs) (Brock and Brock, 1959; Menninger et al., 1994; Taubman et al., 1963). ERY also efficiently inhibits the translation of some synthetic and natural mRNAs in vitro (Otaka and Kaji, 1975; Starosta et al., 2010; Tenson et al., 2003). The presence of ERY in a cell-free system abolishes synthesis of long polypeptides leading instead to production of peptidyl-tRNAs carrying short (4–10 amino acids long) peptides (Otaka and Kaji, 1975; Tenson et al., 2003; Vázquez, 1966).

Mapping the binding site of macrolides in the ribosome has helped to rationalize these observations (Ettayebi et al., 1985; Graham and Weisblum, 1979; Moazed and Noller, 1987) (Figure 1). Macrolides bind in the NPET near the PTC just above the constriction formed by extended loops of ribosomal proteins L4 and L22 (Bulkley et al., 2010; Dunkle et al., 2010; Schlünzen et al., 2001; Tu et al., 2005). Antibiotic binding dramatically narrows the tunnel, thus hindering the progression of the nascent peptide. Therefore, it is generally thought that translation is aborted when the nascent peptide advancing through the NPET reaches the site of antibiotic binding. The notion that a macrolide molecule and an extended nascent chain cannot coexist in the NPET is further supported by the inability of ERY

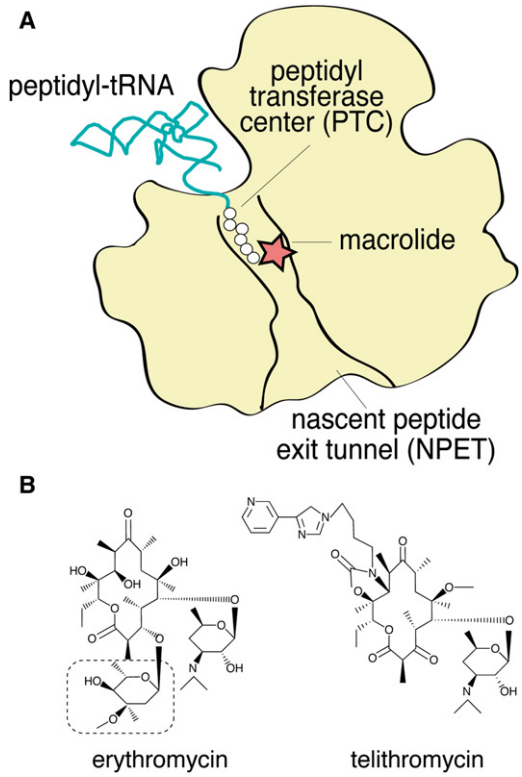

Figure 1. The Macrolide Binding Site in the Large Ribosomal Subunit
(A) Binding of the macrolide antibiotics in the NPET obstructs the progression of the nascent peptide.
(B) Chemical structures of ERY and TEL. Cladinose sugar lacking in ketolides is boxed.

to bind to ribosomes carrying long nascent peptides (Andersson and Kurland, 1987; Tai et al., 1974). The "plug-in-the-bottle" model of macrolide action implies that these drugs, like the majority of protein synthesis inhibitors, indiscriminately stop the production of every protein in the cell during the early stages of their synthesis.

However, some of the experimental data were hard to reconcile with the conventional "plug" model (reviewed in Mankin, 2008). The discovery of drug-dependent ribosome stalling during translation of short regulatory peptides controlling expression of macrolide resistance genes raised the possibility of sequence-specific interactions of antibiotics with the nascent peptide (Horinouchi and Weisblum, 1980; Mayford and Weisblum, 1989). This thought was further reinforced by the identification of short peptides, which could cotranslationally evict macrolide antibiotics from the ribosome (Lovmar et al., 2006; Tenson et al., 1996; Tenson and Mankin, 2001). Several reports also indicated that the inhibitory effects of macrolides on translation of individual reporters in a cell-free system may vary (Hardesty et al., 1990; Odom et al., 1991; Starosta et al., 2010; Vázquez, 1966). Furthermore, the conventional model of macrolide action could not adequately explain why the newer generation of antibiotics (ketolides) exhibits improved bactericidal activity against some pathogens (Hamilton-Miller and Shah, 1998; Woosley et al., 2010).

Although the recent crystallographic studies of the ribosome complexed with macrolide antibiotics confirmed the notion that the drug obstructs the NPET (Bulkley et al., 2010; Dunkle et al., 2010; Schlünzen et al., 2001; Tu et al., 2005), the structures showed that the bound macrolide molecule leaves a considerable amount of room in the NPET. Moore, Steitz, and coworkers (Tu et al., 2005) proposed that the residual space could be wide enough to give the nascent peptide an opportunity to slither through. However, it remained unknown whether such an opportunity is ever realized.

In this paper, we demonstrate that macrolides are protein specific rather than general translation inhibitors, because some proteins can escape macrolide action by threading through the drug-obstructed ribosomal tunnel. We further show that macrolides can arrest translation of some proteins at the later stages of polypeptide synthesis by locking long nascent peptides in the NPET. Both the initial protein threading and the late translation arrest critically depend on the structure of the antibiotic, the sequence of the nascent peptide, and the architecture of the NPET itself. Our findings underscore the discriminating properties of the ribosomal exit tunnel and reveal that small-molecule effectors can modulate them.

RESULTS

A Selective Subset of Proteins Is Synthesized in Bacterial Cells Exposed to High Concentrations of Macrolide Antibiotics

To re-evaluate the mode of translation inhibition by macrolides, we monitored the incorporation of radioactive [^{35}S]-methionine into proteins after the exposure of bacteria to an antibiotic. For these experiments, a macrolide-sensitive *Escherichia coli* strain was prepared by inactivating the *tolC* gene. At the minimal inhibitory concentration (MIC) of ERY (1 μg/ml) (Table S1 available online), an expected drop in protein synthesis was observed (Figure 2A). Raising the ERY concentration to nearly 20-fold the MIC correlated with a further decrease in protein synthesis down to 5%–7% of the untreated control. Unexpectedly, however, further increase in the concentration of the antibiotic had little effect on the residual translation: cells exposed to 100-fold the MIC continued to synthesize proteins at ~6% of the level of the control. Even more striking, TEL, the ketolide, known to be a more potent antibiotic than ERY, permitted a much higher level of residual protein synthesis: 20%–25% at 100-fold the MIC. The onset of translation inhibition by macrolides was very rapid and the maximal level of inhibition was achieved as early as 5 min after the addition of the drug; however, substantial residual protein synthesis persisted even after 6 hr of incubation with the antibiotic (Figure 2B).

Persistent translation in the presence of macrolides could be accounted for by the accumulation of short peptidyl-tRNA dropoff products, the low-level expression of all proteins (due to, e.g., an occasional dissociation of the drug from the translating ribosomes; Lovmar et al., 2006), or, alternatively, in a more unconventional scenario, the selective expression of a subset of polypeptides. In order to discriminate between these possibilities, we analyzed the proteins synthesized in bacteria exposed to macrolide antibiotics. Exponentially growing cells

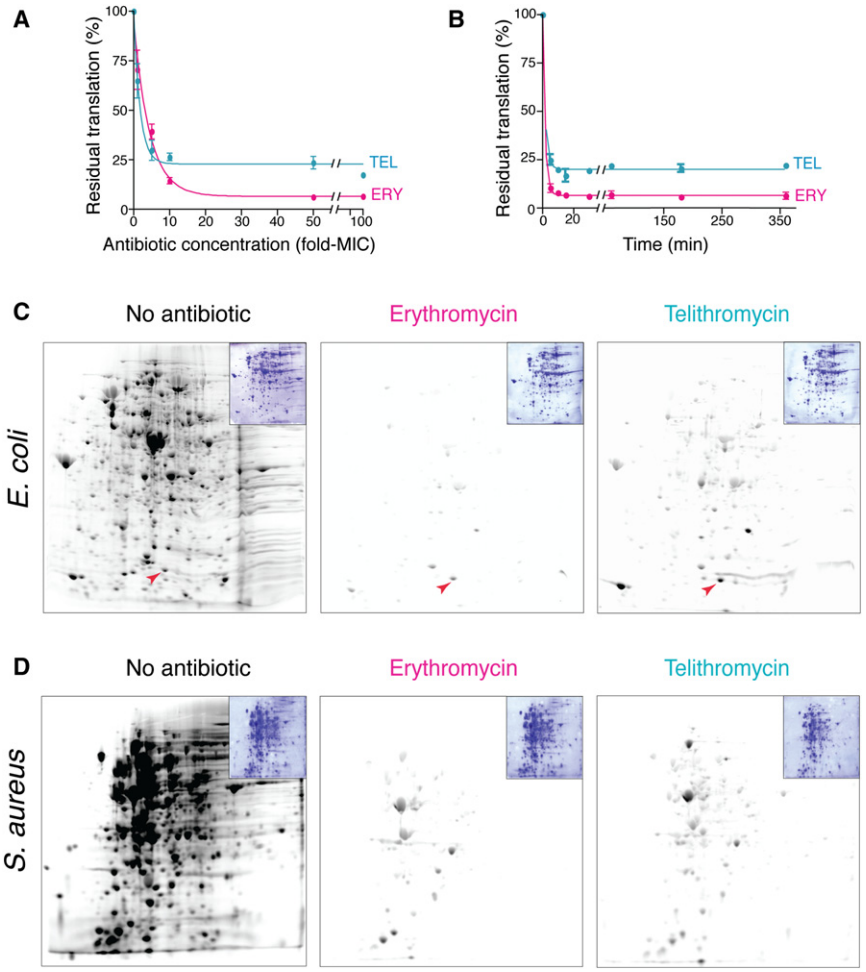

Figure 2. The Selective Translation of Proteins in Cells Exposed to Macrolide Antibiotics

(A) Residual protein synthesis in the presence of increasing concentrations of ERY and TEL. Pulse incorporation of [^{35}S]-methionine in the protein fraction was determined after 15 min exposure of macrolide-sensitive Δ*tolC* *E. coli* cells to varying concentrations of the drugs. Minimal drug inhibitory concentrations Δ*tolC* *E. coli* is 1 μg/ml for ERY and 0.5 μg/ml for TEL (Table S1).

(B) Residual protein synthesis after exposure of *E. coli* cells to the 100-fold MIC of ERY or TEL for varying times. In (A) and (B), the data points represent the mean value of residual translation in two independent experiments with the error bars representing absolute deviation. The correlation coefficient of the graphs fitted into individual data sets is 0.98 for ERY and TEL curves in (A) and 0.99 and 0.95 for ERY and TEL curves, respectively, in (B).

(C and D) Analysis of proteins synthesized in *E. coli* (C) or *S. aureus* str. Newman (D) cells treated with macrolide antibiotics. Pulse-labeled proteins, isolated from cells exposed for 15 min to the 100-fold MIC of ERY or TEL, were resolved by 2D gel electrophoresis. The spots representing the H-NS protein are indicated on the gels by red arrowheads. The Coomassie-stained gels are shown in insets.

See also Figures S1 and S2 and Table S1.

were incubated with 100-fold the MIC of different macrolides for 15 min (Figure 2B). After pulse labeling with [^{35}S]-methionine, the proteins newly synthesized in the presence of the drugs were resolved by 2D gel electrophoresis (Figures 2C, 2D, and S1A). Under these conditions, synthesis of the majority of cellular polypeptides is almost completely inhibited by ERY (Figure 2C) or azithromycin (Figure S1A). However, a small number of labeled protein spots were observed, showing that specific polypeptides continue to be actively synthesized in the presence of the antibiotic, albeit at levels somewhat lower compared to the control cells. The spectrum of proteins synthesized in the presence of the drug remained largely unchanged even after prolonged exposure (up to 6 hr) of cells to the antibiotic (Figure S1B). In agreement with the bulk radiolabel-incorporation experiments (Figures 2A and 2B), the number of resistant proteins and the level of their translation in cells exposed to ketolides, such as TEL and solithromycin, was higher than in cells treated with ERY or azithromycin (Figures 2C and S1A). Although some proteins were resistant to all the macrolides tested (Figure S2A, green circles), many polypeptides exhibited drug-specific resistance (Figure S2A, blue and magenta circles). It appears that the chemical structure of the drug bound in the NPET defines the spectrum of the resistant polypeptides. In contrast to macrolides, chloramphenicol, which binds at the PTC, efficiently inhibited synthesis of all cellular proteins (Figure S1C). The protein-specific inhibitory action of macrolides was not limited to the Gram-negative *E. coli*, but was also observed in the Gram-positive pathogen *Staphylococcus aureus* str. Newman (Figure 2D), demonstrating the general nature of the phenomenon.

The N-Terminal Sequence Defines the Protein's Ability to Evade Inhibition by Macrolide Antibiotics

To gain insights into the molecular mechanisms of drug evasion by selected proteins, we examined how ERY affects the translation of individual polypeptides in vitro. We first identified some proteins synthesized in *E. coli* cells exposed to macrolides. Several spots from the 2D gels (Figure 2C) with the highest relative radioactivity and electrophoretic mobility similar to the untreated control were excised and analyzed by mass spectrometry. After discarding the proteins with low confidence scores and spots with ambiguous identity assignments, we were able to positively identify seven proteins that were resistant to ERY and 18 that were resistant to TEL (Figure S2A).

Four of the ERY-resistant polypeptides corresponded to the secreted outer membrane (OmpX, Tsx, BamA) or inner membrane (PspA) proteins whose translation is difficult to reproduce faithfully in the cell-free system. Of the three remaining cytosolic proteins, we chose for the subsequent in vitro experiments the small cytoplasmic protein H-NS (16 kDa), which was expressed

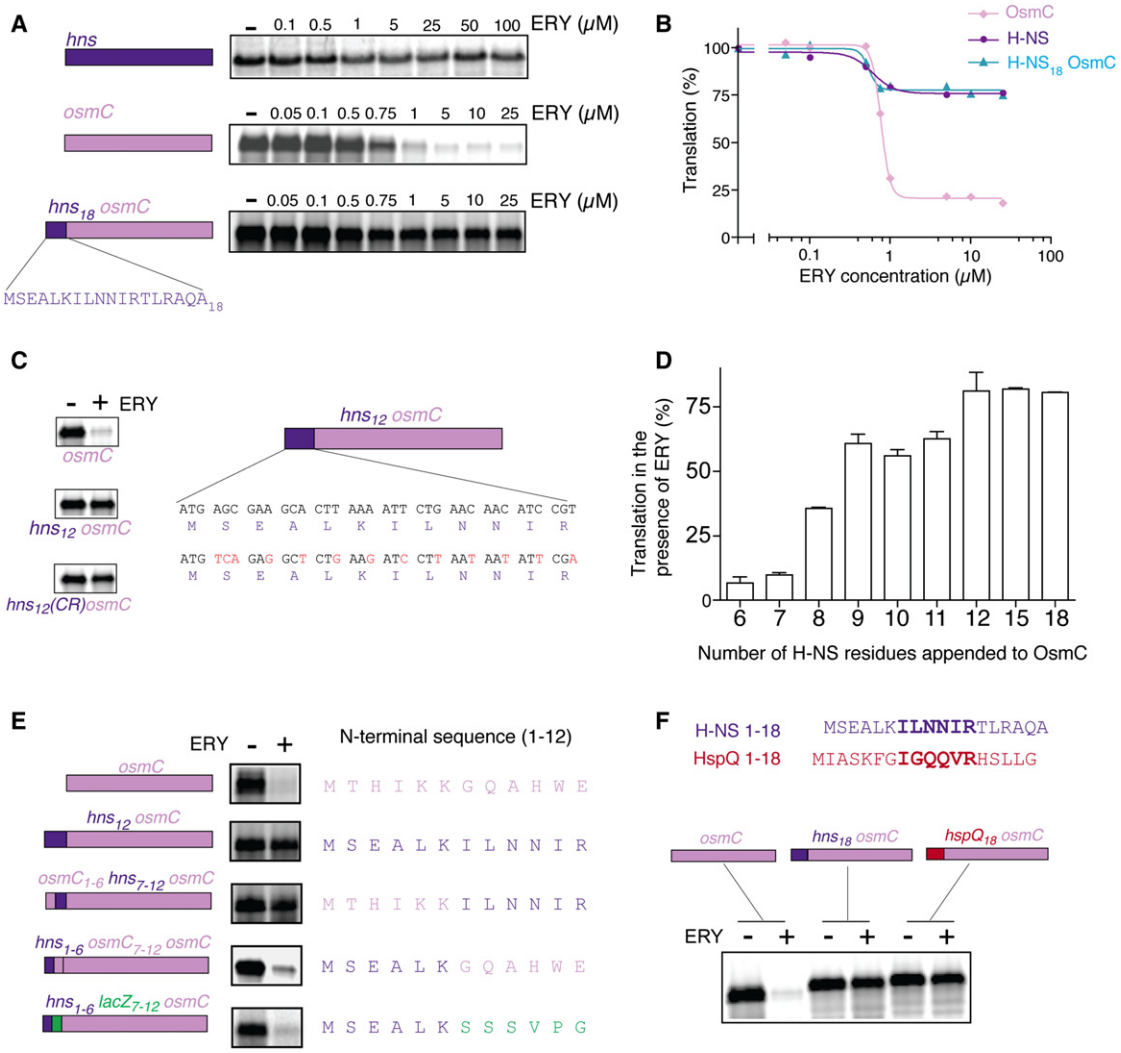

Figure 3. The N-Terminal Amino Acid Sequence of H-NS Renders Proteins Resistant to ERY

(A) The effect of increasing concentrations of ERY on cell-free translation of H-NS, OsmC, and the H-NS$_{18}$OsmC hybrid. Shown gel bands represent the full-size [^{35}S]-labeled proteins resolved by SDS gel electrophoresis.

(B) Quantification of the bands from gels in (A).

(C) Synonymous codon substitutions within the twelve 5′-terminal *hns* codons of *hns$_{12}$osmC* do not diminish ERY resistance of the hybrid protein in the cell-free translation system. The nucleotide substitutions in the codon-replacement construct, *hns$_{12}$(CR)osmC*, are shown in red.

(D) ERY resistance depends on the number of the N-terminal H-NS amino acid residues appended to OsmC. The hybrid proteins were translated in the *E. coli* S30 cell-free translation system in the absence or the presence of 50 μM ERY. The bars represent the mean value of residual translation in two independent experiments with the error bars representing absolute deviation. The correlation coefficient of two individual data sets was 0.97.

(E) ERY sensitivity of the *hns$_{12}$osmC* hybrid constructs with different replacements within the N-terminal sequence appended to OsmC. The sequences of 12 N-terminal amino acids are shown at the right. The gels show the full-size hybrid proteins translated in vitro in the absence or the presence of 50 μM ERY.

(F) N-terminal segment of the *E. coli* protein HspQ (red), that exhibits similarity to H-NS (purple) renders OsmC resistant to ERY. The sequences of H-NS residues 7–12 and HspQ residues 8–13 are shown in bold. The gel shows the [^{35}S]-labeled translation products corresponding to the full-size proteins accumulated in cell-free translation system in the absence (–) or presence (+) of 50 μM ERY.

See also Figure S3.

in cells treated with all of the tested macrolides (arrowheads in Figures 2C and S1A). As a control, we used an ERY-sensitive cytoplasmic protein of comparable size, OsmC (15 kDa). While the synthesis of OsmC in the *E. coli* S30 cell-free system was readily inhibited by ERY (IC_{50} = 0.8 ± 0.3 μM), translation of *hns* was only marginally affected even at higher concentrations of antibiotic, thereby recapitulating the in vivo results (Figures 3A and 3B).

The N terminus of H-NS is the first to encounter the antibiotic in the NPET and therefore may account for the ability of the protein to evade the macrolide inhibitory action. We test this idea by fusing the first 18 codons of *hns* to the 5′ end of the *osmC*

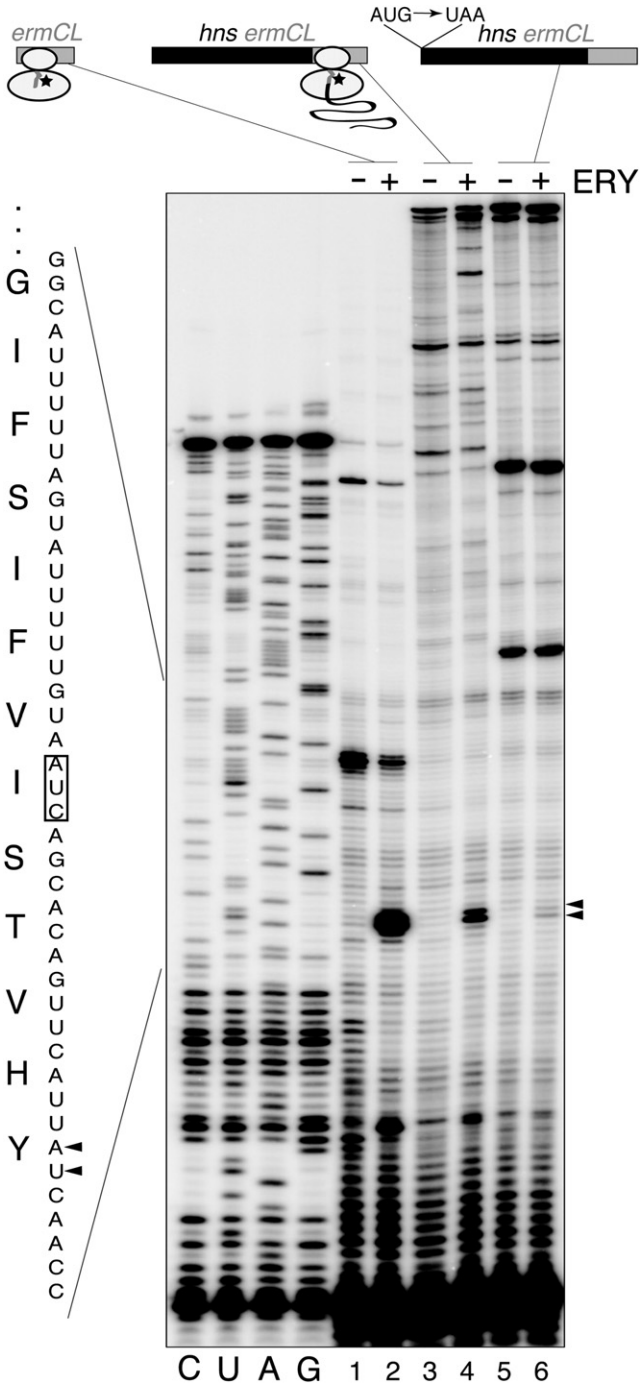

Figure 4. ERY Is Retained in the NPET of the Ribosome Synthesizing the H-NS Protein

Toe-printing analysis of ERY-dependent ribosome stalling within the ErmCL coding sequence. The 19 codon *ermCL* gene (lanes 1 and 2) or the hybrid *hns-ermCL* constructs (lanes 3 and 4, hybrid with a wild-type *hns* start codon; lanes 5 and 6, hybrid with the mutated *hns* start codon) were translated in the cell-free translation system in the absence (lanes 1, 3, and 5) or presence (lanes 2, 4, and 6) of ERY (50 μM). Ribosome stalling within the *ermCL* sequence was detected by primer extension. The bands representing ribosome stalled within the *ermCL* sequence are indicated by triangles and the *ermCL* codon in the P-site of the stalled ribosome is boxed. The very weak toeprint bands in the start codon mutant sample (lane 6) are likely explained by low-frequency translation initiation at one of the internal AUG codons of *hns*. The cartoons above the gel represent the *ermCL* (gray bars) and *hns* (black bar) ORFs with ERY shown as a star.

gene and analyzing the translation of the chimeric protein in the S30 cell-free system in the presence of ERY. The H-NS N terminus rendered OsmC highly resistant to the drug (Figures 3A and 3B). The resistance of H-NS_{18}OsmC to ERY was retained when multiple synonymous codon replacements were introduced in the *hns* segment of the hybrid mRNA (Figure 3C). This result indicates that the ability to elude the drug action is associated with the nascent peptide, rather than with the mRNA structure. In order to better define the amino acid sequence sufficient for drug evasion, we appended varying number of H-NS N-terminal residues to OsmC (Figure 3D). Resistance to the antibiotic started to increase when seven or more amino acids were added and saturated upon the addition of 12–15 H-NS residues. Thus, the resistance determinant resides primarily within the M_1SEALKILNNIR_{12} N-terminal amino acid segment of H-NS. Substituting amino acid residues 1–6 with different amino acids had little effect (Figure 3E). However, replacing the I_7LNNIR_{12} segment of H-NS with the sequence from the susceptible proteins such as LacZ (S_7SSVPG_{12}) or OsmC (G_7QAHWE_{12}) abolished resistance to ERY (Figure 3E). Appending the MSEALKILNNIR sequence to the OsmC N terminus increased its resistance to ERY not only in vitro, but also in vivo (Figure S3).

We searched the *E. coli* proteome for polypeptides whose N-terminal structure resembles that of H-NS (Kanehisa et al., 2002). The protein HspQ carries at its N terminus the sequence I_8GQQVR_{13} whose physicochemical properties are comparable to the critical sequence I_7LNNIR_{12} of H-NS. Similar to *hns*, the in vitro translation of *hspQ* continued at a high ERY concentration (data not shown). Furthermore, the 18 amino acid N-terminal segment of HspQ appended to OsmC rendered the hybrid protein resistant to the drug (Figure 3F). This result reiterated the notion that idiosyncratic properties of the N terminus can render a protein resistant to macrolide antibiotics.

Nascent Peptides Can Bypass the Antibiotic Molecule in the Ribosomal Tunnel

Different scenarios may account for the ability of a protein to escape the inhibitory action of macrolides. The N termini of some nascent peptides could displace the drug from the NPET (Lovmar et al., 2006; Tenson et al., 1997). The nascent peptide elongated by a few more amino acids would then prevent the rebinding of the antibiotic until the completed polypeptide is released from the ribosome. An alternative scenario is that some nascent peptides could sneak through the drug-obstructed NPET without displacing the antibiotic. In order to assess which of these mechanisms accounts for the resistance of H-NS to macrolides, we exploited the phenomenon of ERY-dependent ribosome stalling. The 19 codon open reading frame (ORF) *ermCL* regulates the expression of the macrolide resistance gene *ermC* via programmed translation arrest (Weisblum, 1995). When ERY is bound in the NPET, the ribosome stalls after polymerizing the ErmCL nascent peptide MGIFSIFVI but no translation arrest takes place in the absence of the drug (Figure 4,

lanes 1 and 2) (Horinouchi and Weisblum, 1980; Mayford and Weisblum, 1989; Vázquez-Laslop et al., 2008). We fused codons 2–19 of *ermCL* at the 3′ end of the *hns* gene and tested whether the ribosome would stall after reaching the *ermCL* segment of the hybrid *hns-ermCL* construct (Figure 4). Primer extension inhibition analysis ("toe-printing") (Hartz et al., 1988) yielded the characteristic band on the gel indicative of the antibiotic-dependent translation arrest within the *ermCL* gene (Figure 4, lane 4). Little to no ribosome stalling was observed in the absence of the drug or when the start codon of the *hns-ermCL* fusion was mutated (Figure 4, lanes 3, 5, and 6). This result demonstrated that ribosomes that have translated the entire H-NS protein followed by the ErmCL segment GIFSIFVI retained the ERY molecule bound in the NPET. Because the ribosome carrying a long nascent peptide is presumed to be refractory to ERY rebinding (Pestka, 1972; Tai et al., 1974), the most likely explanation of our results is that the N terminus of the H-NS nascent peptide threads through the NPET obstructed by the antibiotic.

Selective Discriminating Effects of Macrolide Antibiotics at the Late Elongation Stages of Protein Synthesis

Since the opening of the NPET is severely occluded by the macrolide molecule, negotiating the narrowed tunnel could be problematic for some natural nascent peptide sequences even after the initial N-terminal bypass. In order to test whether the macrolide drug can render the ribosome discriminating at the later stages of elongation, we analyzed synthesis of several polypeptides in the S30 cell-free translation system in the presence of saturating concentrations (50 μM) of TEL. (This ketolide allows the synthesis of a larger number of proteins compared to ERY [Figure 2C], suggesting that more polypeptides would be able to avoid inhibition at the early rounds of their synthesis.) From a limited set of examined proteins, the synthesis of the 78 kDa translation elongation factor EF-G (encoded by *fusA*) exhibited an unusual trait. When *fusA* was translated in the presence of the antibiotic, synthesis of the full-size EF-G was abolished and, instead, a polypeptide with an apparent molecular weight of 40 kDa was generated (Figure 5A). The same product appeared in the presence of TEL when the 3′-truncated versions of the *fusA* gene were used as a template indicating that the drug-induced 40 kDa product corresponds to the N-terminal segment of EF-G (Figure 5B). This result showed that the ribosome with the antibiotic molecule bound in the NPET retains its discriminating properties long after the initial encounter of the nascent peptide with the drug.

The precise site of TEL-dependent translation arrest in the *fus*A gene was determined by toe-printing. A unique strong band was observed on the gel in the TEL-containing sample, indicative of drug-dependent translation arrest at the Glu_{358} codon of *fus*A (Figure 5C, lane 2). No ribosome stalling was observed when the start codon of *fusA* was disabled by a mutation (Figure 5C, lane 4). Therefore, ribosomes stalled by TEL at the 358th codon of the wild-type *fusA* gene should carry a 358-amino-acid-long nascent peptide.

We further tested whether other macrolide antibiotics can trigger late translation arrest. To this end, we analyzed in vitro translation of the 57 kDa protein firefly luciferase (Luc) in the presence of ERY. Translation of wild-type *luc* is highly sensitive to ERY and is completely inhibited when the drug concentration exceeds 1 μM (Figures S4A and S4C). Contrary to the ERY-resistant H-NS_{18}OsmC (Figure 3A), appending the 18 N-terminal amino acids of H-NS to luciferase failed to rescue the hybrid protein from antibiotic inhibition (Figures S4B and S4D). Instead, translation of the *hns_{18}luc* led to drug-dependent accumulation of a polypeptide with an apparent molecular weight of 20 kDa (Figure 5F). This shows that the H-NS_{18}Luc N terminus was able to bypass ERY in the NPET, but that translation of the protein was arrested after the synthesis of an ~180-amino-acid-long nascent peptide. In agreement with this notion, the addition of 18 N-terminal amino acids of another ERY-resistant protein, OmpX, at the beginning of luciferase resulted in the accumulation of the same 20 kDa product in the presence of ERY (Figure S5D).

Toe-printing analysis revealed formation of ERY-dependent stalled ribosome complexes at codons Pro_{189}, Pro_{199}, and Asp_{205} of the *hns_{18}luc* hybrid gene (Figure 5G, lane 2). The start codon mutation (Figure 5G) and the fusion of the hybrid template with the *ermCL* reporter (Figures S5A and S5B) demonstrated that ERY remains bound in the NPET of the ribosome that comes to a stall after polymerizing a large fragment of the H-NS_{18}Luc protein. These results confirmed that, similar to ketolides, cladinose-containing macrolides can arrest translation long after the initial threading of the nascent peptide's N terminus past the antibiotic.

After the N-terminal bypass, the chances for the drug-bound ribosome to encounter a problematic nascent peptide sequence should increase with the length of a polypeptide. Indeed, the size distribution of the proteins synthesized in the presence of macrolides is shifted toward lower molecular weights compared to the no drug control (Figure S2B). The spectra and abundance of the truncated proteins generated via the N-terminal bypass and late arrest are yet to be determined. However, the appearance of a number of new protein spots upon exposure of cells to TEL (Figure S2C) argues that a considerable fraction of truncated polypeptides can be generated in the bacterial cell during treatment with some macrolide antibiotics.

Antibiotic-Induced Ribosome Stalling Depends on the Structure of the Nascent Peptide

In the stalled ribosome complex, four to five C-terminal amino acid residues of a nascent peptide are able to directly interact with the macrolide antibiotic (Tu et al., 2005; Vázquez-Laslop et al., 2008, 2011a) and may play an important role in the late translation arrest. To test whether the peptide structure defines the site of late arrest, we modified the sequence of ten EF-G amino acids (residues 348–357) at the site of TEL-dependent arrest (Figure 5D). The alteration in the nascent peptide structure was introduced by compensatory frameshift mutations in the *fusA* gene, which changed the sequence of this segment of EF-G with a minimal effect upon the structure of mRNA. This change in the structure of the nascent peptide prevented TEL-dependent ribosome stalling at the Glu_{358} codon of *fus*A. (The synthesis of the full-size EF-G was not completely restored because the alleviation of stalling at the Glu_{358} codon unmasked downstream late-arrest sites leading to the production of a longer, yet incomplete protein [Figure 5D].)

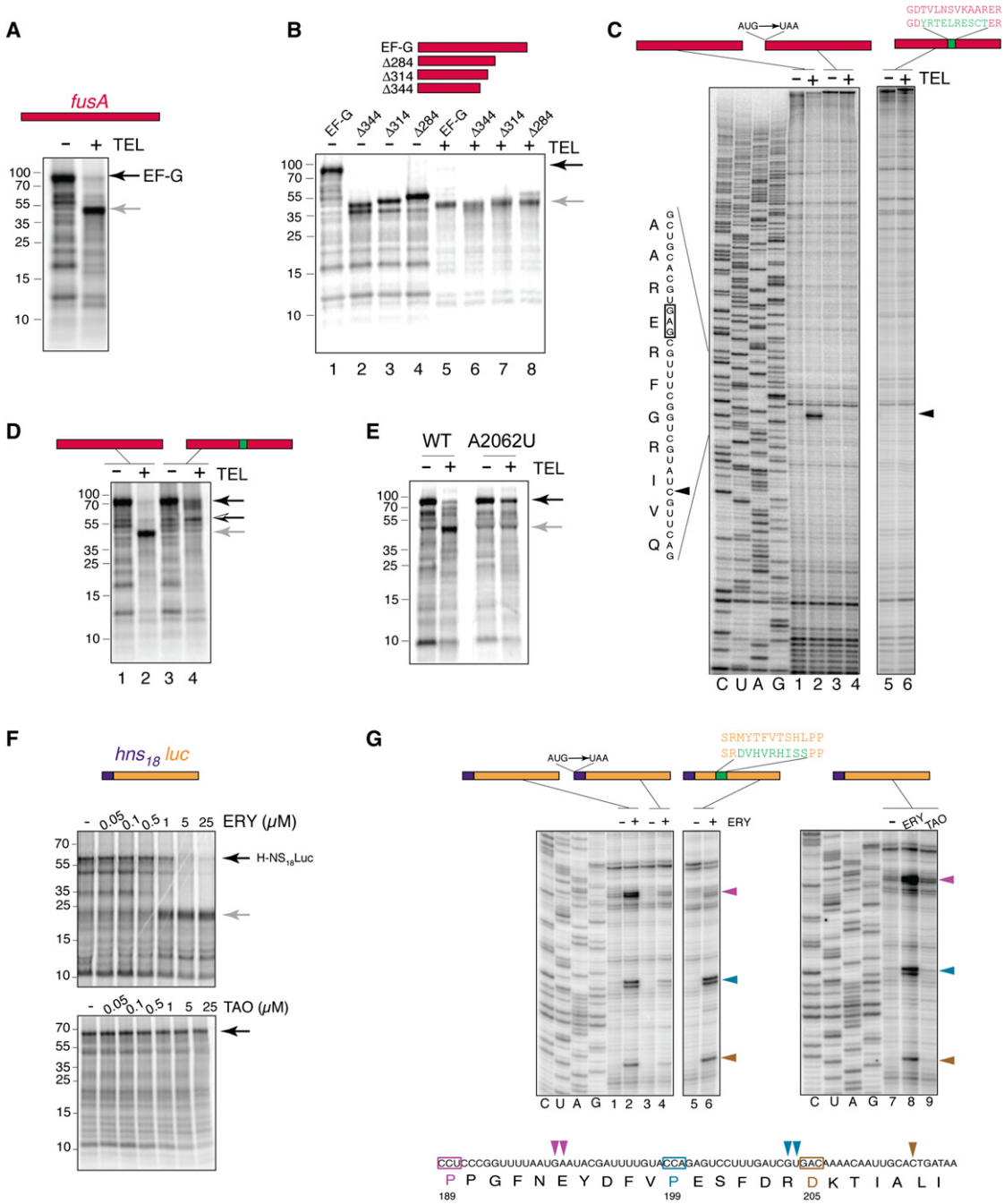

Figure 5. Selective Late Translation Arrest Induced by Macrolide Antibiotics

(A) TEL-dependent arrest of *fusA* translation in the cell-free system. The *fus*A gene was translated in vitro in the absence or presence of 50 μM TEL and the reaction products were resolved by SDS gel electrophoresis. The full-length EF-G and the truncated translation product are indicated by black and gray arrows, respectively, in (A), (B), (D), and (E).

(B) Translation of EF-G and its C-terminally truncated mutants in the absence (−) or presence (+) of TEL. The number of deleted C-terminal residues is indicated.

(C) Detection of the site of TEL-dependent ribosome stalling in the *fusA* gene by toe-printing. The wild-type *fusA* gene (lanes 1 and 2), the start codon mutant (lanes 3 and 4) and the frameshift mutant in which the amino acid residues 348-357 were changed (lanes 5 and 6) were used as templates in a cell-free translation reaction in the absence (−) or presence (+) of 50 μM TEL. Ribosome stalling was detected by primer extension. The toe-printing band is indicated by a triangle and the *fusA* codon (Glu_{358}) located in the P-site of the stalled ribosome is boxed.

(D) SDS gel electrophoresis analysis of the products of in vitro translation of wild-type *fusA* (lanes 1 and 2) or the frameshift mutant (lanes 3 and 4) in the absence or presence of TEL. A new TEL-dependent incomplete translation product of the frameshift mutant is indicated by a bicolored arrow.

(E) The A2062U mutation reduces efficiency of TEL-dependent late translation arrest. SDS gel electrophoresis analysis of the products of translation of *fusA* by wild-type or mutant (A2062U) ribosomes in the absence or presence of a saturating concentration of TEL (50 μM).

ERY-dependent late translation arrest within the *hns18-luc* open reading frame occurs at three sites: Pro_{189}, Pro_{199}, and Asp_{205}. (Figure 5G, lane 2). When a compensatory frameshift mutation altered the residues 180–188 of the H-NS_{18}Luc nascent peptide, ribosome stalling at the Pro_{189} codon was dramatically reduced (Figure 5G, lane 6). In contrast, translation arrest at the two downstream sites, Pro_{199} and Asp_{205}, was not affected. These results demonstrate that late translation arrest depends on the nascent peptide structure and occurs when a "problematic" amino acid sequence advances from the PTC into the NPET.

The Structure of the NPET-Bound Antibiotic Influences the Late Translation Arrest

The structure of the macrolide molecule may impact the efficiency and selectivity of the late translation arrest (Vázquez-Laslop et al., 2011b; Weisblum, 1995). In order to test this concept, we compared the ability of five different macrolides to trigger late ribosomal stalling at the *hns_{18}luc* mRNA. Although all these antibiotics readily inhibited in vitro translation of the wild-type luciferase only four of the five tested macrolides (ERY, clarithromycin, TEL, and CEM-112) promoted the accumulation of a 20 kDa late-arrest translation product (Figure S4F). No truncated polypeptide product was observed in the presence of troleandomycin (Figures 5F and S4F), and, as a result, this drug had little effect on expression of the functionally active enzyme from the *hns_{18}luc* template (Figure S4D). Toe-printing confirmed that the efficiency of troleandomycin-dependent ribosome stalling was dramatically reduced compared to ERY (Figure 5G, lanes 8 and 9). The use of the C-terminal ErmCL reporter showed that troleandomycin remains bound to at least a fraction of the translating ribosomes (Figure S5C). We concluded that changes in the structure of the NPET-bound antibiotic may affect the sequence specificity of late translation arrest.

The Efficiency of Late Ribosome Stalling Depends on the Structure of the Exit Tunnel

The shape of the NPET opening is likely critical for the progression of the newly synthesized protein. Therefore, we tested whether alterations in the NPET structure would affect the nascent peptide-discriminating properties of the drug-bound ribosome. For that, the *fus*A gene was translated in a cell-free system by either wild-type ribosomes or ribosomes carrying the 23S ribosomal RNA (rRNA) mutation A2062U (Figure S6A). Although this mutation did not confer TEL resistance (Table S1) or prevent antibiotic binding (Figure S6C), it significantly reduced the accumulation of the TEL-dependent 40 kDa truncated product, consequently increasing the amount of full-size EF-G (Figure 5E). Furthermore, the spectra of ERY-resistant proteins synthesized in wild-type cells and in mutants with tunnel mutations A2062G or U2609C showed considerable variation (Figure S6B). Altogether, these results demonstrate that the NPET structure directly influences the selective translation properties of the antibiotic-bound ribosome.

DISCUSSION

Discriminating properties of the NPET allow the ribosome to modulate its functions in a protein-specific manner, depending on the nascent peptide sequence (Nakatogawa and Ito, 2002). In this paper, we show that small molecules can globally influence the differentiating capacity of the ribosomal tunnel.

For a long time, macrolide antibiotics have been considered to be general inhibitors of translation that prevent the synthesis of all cellular proteins by plugging the ribosomal tunnel. In contrast to this prevailing view, we demonstrated that the mode of action of these drugs is protein specific.

With the macrolide antibiotic bound in the NPET, the structure of the nascent peptide N terminus determines whether protein synthesis is aborted, stalled, or continued. When the protein chain grows to five to ten amino acids and reaches the site of the antibiotic binding in the NPET, translation of many polypeptides is aborted because the peptidyl-tRNA dissociates from the ribosome (Menninger, 1995; Tenson et al., 2003) (Figure 6A). A small number of specific short nascent peptides, like those encoded in the regulatory cistrons of macrolide resistance genes, can instead stall the ribosome, which retains peptidyl-tRNA but is unable to catalyze the peptide bond formation (Horinouchi and Weisblum, 1980; Ramu et al., 2011; Vázquez-Laslop et al., 2008). In either of these scenarios, the nascent chain cannot bypass the antibiotic obstacle in the NPET, and protein expression is curtailed. However, due to the phenomenon of the N-terminal bypass, some peptide sequences have the ability to thread through the antibiotic-occupied NPET (Figure 6A), leading to the synthesis of long polypeptides on drug-bound ribosomes.

Crystallographic structures of ribosome-macrolide complexes show that macrolides do not completely block the tunnel, but leave an opening that may provide a passage for the nascent peptide (Figures 6B and 6D) (Bulkley et al., 2010; Dunkle et al., 2010; Schlünzen et al., 2001; Tu et al., 2005). With limited gymnastics, even the bulkiest amino acid residues could pass through the constriction of the drug-obstructed NPET. The aperture of the opening is controlled by the placement of a highly flexible rRNA residue A2062 (Fulle and Gohlke, 2009; Seidelt et al., 2009; Vázquez-Laslop et al., 2008). In the absence of a nascent peptide, A2062 comes into close contact with the macrolide

(F) ERY-induced late translation arrest within the *hns_{18}luc* chimeric gene. SDS gel electrophoresis analysis of the products of translation of the *hns_{18}luc* template in the presence of increasing concentrations of ERY (top gel) or troleandomycin (bottom gel). The full-size protein is indicated by the black arrow; the ERY-induced truncated polypeptide is indicated by the gray arrow.

(G) Mapping the sites of ERY-dependent late translation arrest in the *hns_{18}luc* gene. The *hns_{18}luc* template (lanes 1, 2, and 7–9), the start codon mutant (lanes 2 and 4) and the frameshift mutant in which the amino acid residues 180–188 were changed (lanes 5 and 6) were translated in a cell-free system in the absence (lanes 1, 3, 5, and 7) or the presence of ERY (lanes 2, 4, 6, and 8) or troleandomycin (lane 9), and the site of ribosome stalling was analyzed by primer extension. Three prominent stalling sites are indicated by purple, blue, and brown triangles; the codons in the P-site of the corresponding stalled ribosomal complexes are boxed with the same color in the *luc* sequence shown below.

See also Figures S4, Figures S5, and Figures S6.

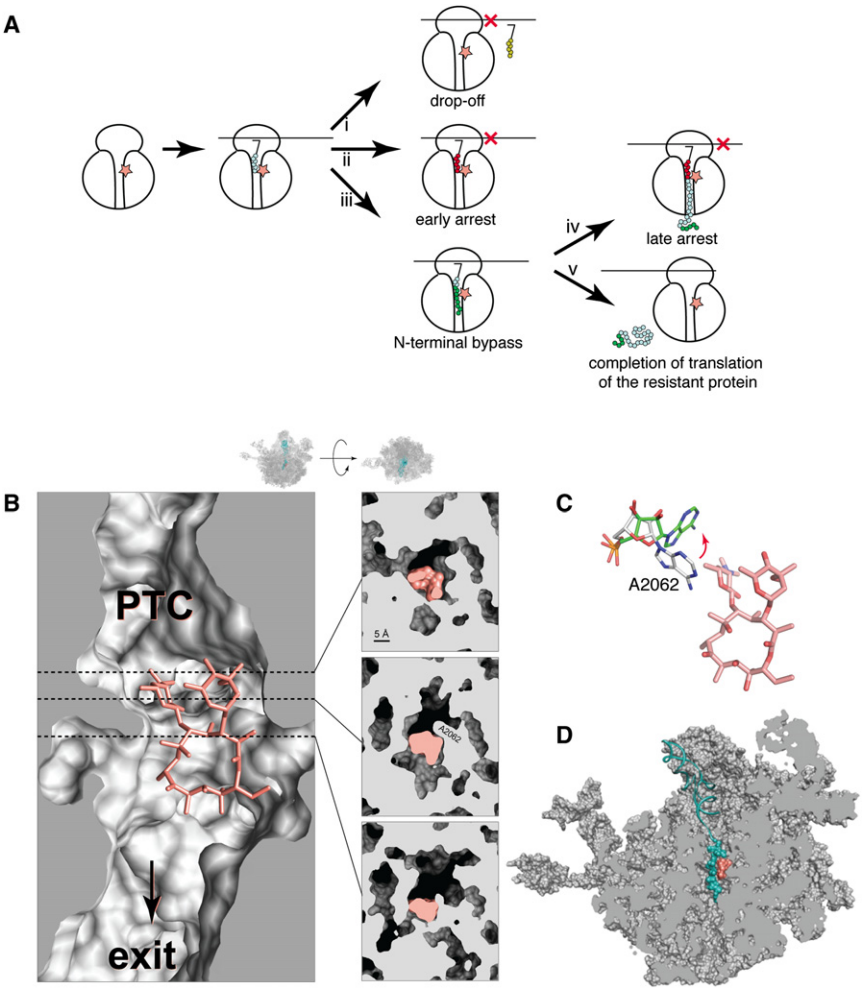

Figure 6. The Mode of Binding and Action of Macrolide Antibiotics

(A) Previously known and new modes of action of macrolide antibiotics. (1) The dropoff of peptidyl-tRNA at the early rounds of translation. (2) Early ribosome stalling (e.g., during translation of regulatory peptides controlling macrolide resistance genes). (3) N-terminal bypass. (4) Late arrest after the N-terminal bypass. (5) Expression of the full-size protein by the drug-bound ribosome. The nascent peptide N-terminal sequence prone to dropoff is shown in yellow, the N-terminal bypass-promoting sequence is green and the peptide segments directing early or late translation arrest are red. The macrolide antibiotic is shown as a star.

(B) The macrolide molecule leaves sufficient space for the nascent peptide in the NPET. The cross-cut of the NPET along the tunnel axes (left) and perpendicular to the tunnel axes (right) of the *E. coli* ribosome complexed with ERY (Protein Data Band ID Code [PDB] 3OFR) (Dunkle et al., 2010). ERY is colored in salmon and the position of the perpendicular cross-cut planes relative to the drug are shown by dotted lines.

(C) Gating of the drug-obstructed tunnel by A2062. In the absence of the nascent peptide, A2062 comes into a close contact with the macrolide narrowing the opening of the NPET (gray carbon atoms, PDB 3OFR; Dunkle et al., 2010). In the presence of the nascent peptide, the residue can potentially reorient to open up the tunnel space. The orientation shown for A2062 (green carbon atoms) corresponds to the placement of the residue in the *Haloarcula marismortui* large ribosomal subunit complexed with the transition state analog (PDB 1VQ7; Schmeing et al., 2005).

(D) Possible simultaneous placement of a macrolide and nascent peptide in the NPET. A cross-cut of the large ribosomal subunit complexed with ERY (salmon) with the modeled 12-amino-acid-long nascent peptide esterifying the P-site tRNA (cyan). See also Figure S6.

molecule, occluding the tunnel lumen (Figures 6B and 6C) (Tu et al., 2005). Some nascent peptides might force the A2062 base to reposition closer to the NPET wall, which would open a larger space in the NPET facilitating the passage of the polypeptide chain (Schmeing et al., 2005) (Figure 6C). The important role of A2062 in nascent peptide surveillance is further emphasized by the fact that its mutation alleviates both early ERY-dependent ribosome stalling at the regulatory ORFs of macrolide resistance genes (Vázquez-Laslop et al., 2008, 2010), as well as TEL-dependent late translation arrest within the *fusA* gene (Figure 5F).

In addition to gating the tunnel, A2062, which may allosterically influence the catalytic properties of the PTC in a peptide-dependent manner (Vázquez-Laslop et al., 2008, 2010), could play a role in the kinetic control of the N-terminal bypass. When the short nascent peptide reaches the tunnel constriction formed by the antibiotic and A2062, subsequent events likely depend on the relative rates of peptidyl-tRNA dropoff, dissociation of the drug, or threading of the peptide through the opening of the antibiotic-obstructed tunnel. It is conceivable that slowing down peptide bond formation in response to specific nascent peptide sequences can abort translation via peptidyl-tRNA dropoff or ribosome stalling. Alternatively, if peptide elongation is kinetically favored, threading the peptide through the tunnel constriction would aid the retention of peptidyl-tRNA in the ribosome, and translation would continue on the drug-bound ribosome. In this regard, it is noteworthy that the bypass directed by the N terminus of H-NS is much more pronounced in the "fast" S30 cell-free translation system compared to the less efficient in vitro system prepared from purified components (Hillebrecht and Chong, 2008).

The protein's N terminus determines its ability to bypass the macrolide molecule and the A2062 gate in the NPET. The broad functional spectrum of macrolide-resistant proteins (Figure S2A) argue that it is the local structure of the N-terminal sequence rather than protein function that defines the propensity for the bypass. As few as 12 N-terminal amino acids of H-NS (MSEALKILNNIR) are sufficient for rendering a macrolide-sensitive protein (OsmC) highly resistant to the drug. Within the H-NS N-terminal structure, the first six N-terminal amino acids appear

to be fairly inconsequential whereas the segment I_7LNNIR$_{12}$ plays more important role in antibiotic evasion because its replacement with an unrelated sequence dramatically reduced the N-terminal threading capacity (Figure 3E). In contrast, alanine substitutions of individual amino acids had little effect on bypass (data not shown). Either a particular folding of this segment or the cumulative effects of specific contacts of several amino acid residues with the ribosome and/or the antibiotic appear to be required for efficient threading of the peptide through the drug-obstructed tunnel. Any of these mechanisms may either orient the peptide's N terminus for slithering through the narrow gap of the antibiotic-occupied NPET or modify the shape of the tunnel (e.g., inducing the reorientation of A2062) and/or the pose of the antibiotic, thereby facilitating the bypass. In the mature H-NS protein, the I_7LNNIR$_{12}$ sequence folds into a unique "kinked" α helix stabilized by interactions with the second H-NS molecule (Bloch et al., 2003). It is unlikely, however, that such a structure is possible within the confines of the NPET.

None of the N-terminal sequences of the other ERY- or TEL-resistant proteins that we identified in the 2D gel spots (Figure S2A) closely matches that of H-NS. Therefore, it is obvious that the sequence constraints for the N-terminal bypass are fairly relaxed, especially in the case of ketolides, which allow the escape of many more polypeptides. We noted, however, that N-terminal segments of several of the resistant proteins contain a stretch of two to three hydrophobic residues followed by a positively charged amino acid (underlined in Figure S2A). It remains to be determined whether this feature is one of the drug-evasion determinants.

The presence of an antibiotic molecule in the NPET renders the ribosome selective not only at the beginning of protein synthesis, but also during later stages of the nascent peptide polymerization. Following the N-terminal bypass, translation of some polypeptides can continue unimpeded, whereas elongation of other proteins can be arrested at a subsequent phase, leading to the phenomenon of macrolide-dependent late translation arrest. Similar to the N-terminal bypass, the structure of the nascent peptide, and more specifically of its PTC-proximal segment, is the key factor in defining the site of the late arrest; altering a short C-terminal nascent peptide sequence at the arrest site (Figures 5D and 5H) can alleviate ribosome stalling. Although the molecular mechanism of the late arrest remains to be investigated, we noted that the site of the TEL-dependent arrest within the *fusA* gene (Arg_{357}-Glu_{358}-Arg_{359}, with the Glu codon positioned in the P-site of the stalled ribosome) resembles the conserved motif (Arg-Leu-Arg) of the "RLR" class of short stalling peptides of the inducible macrolide resistance genes (Ramu et al., 2009). It is possible, therefore, that the basic principles of the late translation arrest and the early drug-dependent ribosome stalling are generally similar.

Peptide surveillance properties of the ribosome are directly affected by the structure of the tunnel-bound small-molecule effectors. Ketolides, which lack the bulky C3 cladinose, permit the synthesis of many more proteins than cladinose-containing macrolides (Figures 2C, 2D, and S1A). Other variations in the drug structure can also influence the discriminating properties of the NPET (Figures 5G, S4D, and S4F) either directly, by changing the shape of the tunnel aperture and idiosyncratic interactions with the nascent peptide, or by altering the site of the drug binding in the NPET (Berisio et al., 2003). An important concept that emerges from this result is that by modifying the structure of the tunnel-bound antibiotic, or in more general terms, of any small molecule that binds in the NPET, it is possible to deliberately alter the spectra of the proteins translated by the ribosome.

The macrolide-mediated selectivity of translation can be additionally affected by extraribosomal cues. Several secreted proteins, including OmpX, were actively synthesized in *E. coli* exposed to ERY (Figure S2A) but their translation was inhibited in cell-free system. Although fusion of the N-terminal 18 amino acid segment of OmpX to luciferase promoted the N-terminal bypass (Figure S5D), the in vitro translation of the full-size OmpX protein remained sensitive to ERY likely due to late translation arrest (data not shown). Interaction of the OmpX nascent peptide with the cytoplasmic components of the secretion machinery (Huber et al., 2011) and/or the pulling force of the translocon (Chiba et al., 2011; Nakatogawa and Ito, 2002) could facilitate the bypass of the late-arrest site(s), thus ensuring the successful elongation of the membrane protein in vivo.

The selective N-terminal bypass and late translation arrest can account for some previously puzzling results. The long-known resistance of polyU translation to ERY (Hardesty et al., 1990; Vázquez, 1966) and a more recently reported poor inhibition of in vitro synthesis of green fluorescent protein (GFP) by macrolides (Starosta et al., 2010) can be easily rationalized if one assumes that poly(Phe) and GFP could thread through the macrolide-occupied NPET. A number of other results, from the accumulation of long peptidyl-tRNA (Menninger et al., 1994; Yao et al., 2008), to the persistence of polysomes in ERY-treated cells (Ennis, 1972), to the ERY resistance caused by ribosomal protein L22 mutations (Apirion, 1967; Chittum and Champney, 1994; Lovmar et al., 2009; Moore and Sauer, 2008), which were hard to explain within the confines of the conventional model of macrolide action, now could be rationalized in view of our findings.

The understanding that macrolides do not block synthesis of all the proteins, but rather convert the universal translation machine into a selective producer of certain polypeptides, has important clinical implications. Ketolides are much more potent antibacterials than the drugs of previous generations. Furthermore, ketolides exhibit increased bactericidal activity against some Gram-positive bacteria (Hamilton-Miller and Shah, 1998; Woosley et al., 2010; Zhanel and Hoban, 2002). Strikingly, ketolides license continued synthesis of by far more proteins than ERY or azithromycin (Figures 2C, 2D, and S1A). It appears that blocking the expression of only a part of the cellular proteome could be more fatal to the cell than a complete or near-complete inhibition of translation. Preventing translation of only a subset of proteins will interrupt biochemical pathways at random steps leading to the accumulation of potentially toxic metabolic intermediates or depletion of essential cofactors, which may trigger a lethal cellular response (Kohanski et al., 2007). In contrast, inhibiting synthesis of all the proteins would eventually deprive the cell from its biosynthetic and metabolic capacity, leading to bacteriostasis. Noteworthy, whereas most of the "global" protein synthesis inhibitors are bacteriostatic, aminoglycosides that permit some protein synthesis but render the ribosome error

prone are strongly bactericidal (Vázquez, 1979). The production of truncated polypeptides generated via late translation arrest could be another important factor contributing to the increased potency of ketolides.

The new insights into the mode of action of macrolide antibiotics offer novel directions for drug discovery. Optimizing the tunnel-bound antibiotics for inhibiting specific proteins may increase the cidality of the drugs, thereby improving the outcomes of antibiotic therapy. Furthermore, identifying small molecules that modulate the translation of individual proteins in the eukaryotic cell by binding in the NPET of the eukaryotic ribosome can find application in broad areas of medicine (Peltz et al., 2009).

EXPERIMENTAL PROCEDURES

Metabolic Labeling of Proteins

The macrolide-hypersusceptible *tolC*$^{-}$ *E. coli* strain BWDK was prepared by curing the resistance marker in the BW25113-derived *tolC*::*kan* strain (Baba et al., 2006). BWDK cells, exponentially growing in 100 μl of M9 medium supplemented with 40 μg/ml of all amino acids except methionine (M9AA-M), were exposed to 1- to 100-fold MIC of each antibiotic (1–100 μg/ml for ERY or 0.5–50 μg/ml for TEL) for 15 min, after which 1 μCi [^{35}S]-methionine (specific activity 1,175 Ci/mmol) was added, and the cells were incubated for one more minute. The proteins were precipitated by adding an equal volume of ice-cold 25% trichloroacetic acid (TCA) containing 2% casamino acids. After incubating for 30 min on ice and then 30 min at 100°C, samples were passed through G4 glass fiber filters. The filters were washed three times with 3 ml of ice cold 5% TCA, and once with 3 ml of acetone and air dried, and the amount of retained radioactivity was determined by scintillation counting. The data were normalized relative to the "no drug" control.

2D-Gel Electrophoresis Analysis of the Radiolabeled Proteins

Exponentially growing cultures (50 ml) of *E. coli* (strain BWDK, M9AA-M medium) or *S. aureus* (strain Newman, CDM-M medium; Hilliard et al., 1999) were incubated with 100-fold MIC of ERY (100 μg/ml for *E. coli*; 25 μg/ml for *S. aureus*), TEL (50 μg/ml for *E. coli*; 12.5 μg/ml for *S. aureus*), azithromycin (100 μg/ml for *E. coli*), or solithromycin (50 μg/ml for *E. coli*) for 15 min. [^{35}S]-methionine (250 μCi, specific activity 1,175 Ci/mmol) was then added, and the cells were incubated for 3 min, followed by the addition of unlabeled L-methionine to final concentration of 80 μg/ml and further incubation for 7 min. The cells were pelleted by centrifugation at 4,000 × *g* for 15 min at 4°C. The *E. coli* cells were lysed by boiling 5 min in buffer containing 60 mM Tris (pH 6.8), 5% SDS, and 10% glycerol. *S. aureus* cells were lysed by incubation in the lysis buffer (Tris-HCl [pH 7.5], 30 mM $MgCl_2$, 30 mM NH_4Cl, 0.1 mg/ml lysostaphin, 100 U of Omnicleave endonuclease (Epicenter) at 37°C for 30 min. The lysates were centrifuged and the supernatant was passed through a 0.22 μm filter. The extracted proteins (600 μg [*E. coli*] or 200 μg [*S. aureus*]) were fractionated by two-dimensional gel electrophoresis (O'Farrell, 1975) at Kendrick Labs, Inc. (Madison, WI). The gels were stained with Coomassie brilliant blue, dried, and exposed to the phosphorimager screen overnight.

Protein Identification

The radiolabeled spots in the 2D gels containing ERY- or TEL-treated samples were computationally correlated with the Coomassie-stained, nonradiolabeled 2D gels. The stained protein spots were cut out and subjected to LC/MS/MS analysis at the Proteomics facility of the University of Illinois at Chicago.

Cell-Free Protein Synthesis and Analysis of Translation Products

In vitro translation was carried out in the *E. coli* S30 cell-free transcription-translation system for linear templates (Promega). PCR-generated DNA template (0.1–0.5 pmol) carrying the desired gene under the control of the P*tac* promoter was translated in a 5 μl reaction containing 2 μCi [^{35}S]-methionine (specific activity 1,175 Ci/mmol) following the manufacturer's protocol. After 30–45 min incubation at 37°C, the reactions were treated with 0.5 μg RNase A for 5 min at 37°C and precipitated with four volumes of ice cold acetone. Proteins were fractionated in a 16.5% polyacrylamide gel using the Tricine-SDS buffer system (Schägger and von Jagow, 1987). Gels were dried and exposed overnight to a phosphorimager screen. The bands were quantified using the ImageJ software (http://rsbweb.nih.gov/ij/). The background intensity was subtracted and the integrated density values were normalized relative to the no-drug control. The normalized band intensity values were fitted to a sigmoidal dose response curve (95% confidence level) using the Prism software (GraphPad).

The activity of in vitro translated firefly luciferase was determined using the Luciferase Assay Reagent (Promega) as recommended by the manufacturer.

Toe-Printing Assay

The toe-printing assay for drug-dependent ribosome stalling was carried out as described (Vázquez-Laslop et al., 2008), with minor modifications. The templates coding for the protein sequences under the control of T7 promoter were generated by PCR. The templates (0.05–0.1 pmol) were used in a total volume of 5 μl of the *E. coli* cell-free transcription-translation system assembled from purified components (New England Biolabs). The reactions were incubated for 15 min at 37°C, followed by addition of the toe-printing primer designed to anneal ~100 nucleotides downstream from the anticipated ribosome stalling site. All the other procedures were carried out as previously described.

Generation of the Tunnel Mutants and Protein Translation by the Mutant Ribosomes

The mutations A2062G and U2609C were introduced in the 23S rRNA gene in the pLK35 plasmid (Douthwaite et al., 1989). The mutant plasmids were transformed into *E. coli* SQ171*ΔtolC* cells (Bollenbach et al., 2009). Plasmid exchange was carried out following Zaporojets et al. (2003) and the mutant ribosomes were prepared as described by Shimizu et al. (2005).

The in vitro translation of the *fus*A or *yib*A genes by wild-type and A2062U mutant ribosomes was carried out in 5 μl reactions (Δribosome PURExpress, New England Biolabs) containing 0.5 pmol of DNA templates and 15 pmol of the ribosomes. After 45 min incubation at 37°C in the presence or absence of TEL (50 μM in the *fus*A-containing reaction or 10 μM during *yib*A expression), the reactions were stopped as described above and analyzed by SDS gel electrophoresis.

For in vivo experiments, *E. coli* SQ171*ΔtolC* cells expressing wild-type or mutant (A2062G or U2609C) ribosomes were grown in 10 ml of M9AA-M media. Exponentially growing cultures were incubated with 100-fold MIC (100 μg/ml) of ERY for 15 min prior to addition of 100 μCi of [^{35}S]-methionine, incubation of 3 min, and the subsequent addition of an excess of L-methionine and incubation for 7 min. Cells were harvested by centrifugation and lysed by boiling in SDS gel loading buffer, and proteins were resolved on 16.5% SDS gel.

SUPPLEMENTAL INFORMATION

Supplemental Information includes six figures and one table and can be found with this article online at http://dx.doi.org/10.1016/j.cell.2012.09.018.

ACKNOWLEDGMENTS

We thank Anusha Rethi Paul Raj, Dorota Klepacki, Anna Ochabowicz, and Jacqueline M. LaMarre for help with experiments, Teymur Kazakov for advice, Prabha Fernandez for providing solithromycin and CEM-112, and Kirk Hevener for advice on using Chimera software. We are grateful to Peter Moore, Harry Noller, and Ada Yonath for their comments on the manuscript. This work was supported by grant MCB-0824739 from the National Science Foundation.

Received: April 23, 2012
Revised: June 18, 2012
Accepted: September 10, 2012
Published: October 25, 2012

REFERENCES

Ackermann, G., and Rodloff, A.C. (2003). Drugs of the 21st century: telithromycin (HMR 3647)—the first ketolide. J. Antimicrob. Chemother. *51*, 497–511.

Andersson, S., and Kurland, C.G. (1987). Elongating ribosomes *in vivo* are refractory to erythromycin. Biochimie *69*, 901–904.

Apirion, D. (1967). Three genes that affect *Escherichia coli* ribosomes. J. Mol. Biol. *30*, 255–275.

Baba, T., Ara, T., Hasegawa, M., Takai, Y., Okumura, Y., Baba, M., Datsenko, K.A., Tomita, M., Wanner, B.L., and Mori, H. (2006). Construction of *Escherichia coli* K-12 in-frame, single-gene knockout mutants: the Keio collection. Mol. Syst. Biol. *2*. http://dx.doi.org/10.1038/msb4100050.

Berisio, R., Schluenzen, F., Harms, J., Bashan, A., Auerbach, T., Baram, D., and Yonath, A. (2003). Structural insight into the role of the ribosomal tunnel in cellular regulation. Nat. Struct. Biol. *10*, 366–370.

Bloch, V., Yang, Y., Margeat, E., Chavanieu, A., Augé, M.T., Robert, B., Arold, S., Rimsky, S., and Kochoyan, M. (2003). The H-NS dimerization domain defines a new fold contributing to DNA recognition. Nat. Struct. Biol. *10*, 212–218.

Bollenbach, T., Quan, S., Chait, R., and Kishony, R. (2009). Nonoptimal microbial response to antibiotics underlies suppressive drug interactions. Cell *139*, 707–718.

Brock, T.D., and Brock, M.L. (1959). Similarity in mode of action of chloramphenicol and erythromycin. Biochim. Biophys. Acta *33*, 274–275.

Bulkley, D., Innis, C.A., Blaha, G., and Steitz, T.A. (2010). Revisiting the structures of several antibiotics bound to the bacterial ribosome. Proc. Natl. Acad. Sci. USA *107*, 17158–17163.

Chiba, S., Kanamori, T., Ueda, T., Akiyama, Y., Pogliano, K., and Ito, K. (2011). Recruitment of a species-specific translational arrest module to monitor different cellular processes. Proc. Natl. Acad. Sci. USA *108*, 6073–6078.

Chittum, H.S., and Champney, W.S. (1994). Ribosomal protein gene sequence changes in erythromycin-resistant mutants of *Escherichia coli*. J. Bacteriol. *176*, 6192–6198.

Douthwaite, S., Powers, T., Lee, J.Y., and Noller, H.F. (1989). Defining the structural requirements for a helix in 23 S ribosomal RNA that confers erythromycin resistance. J. Mol. Biol. *209*, 655–665.

Dunkle, J.A., Xiong, L., Mankin, A.S., and Cate, J.H. (2010). Structures of the *Escherichia coli* ribosome with antibiotics bound near the peptidyl transferase center explain spectra of drug action. Proc. Natl. Acad. Sci. USA *107*, 17152–17157.

Ennis, H.L. (1972). Polysome metabolism in *Escherichia coli*: effect of antibiotics on polysome stability. Antimicrob. Agents Chemother. *1*, 197–203.

Ettayebi, M., Prasad, S.M., and Morgan, E.A. (1985). Chloramphenicol-erythromycin resistance mutations in a 23S rRNA gene of *Escherichia coli*. J. Bacteriol. *162*, 551–557.

Fang, P., Spevak, C.C., Wu, C., and Sachs, M.S. (2004). A nascent polypeptide domain that can regulate translation elongation. Proc. Natl. Acad. Sci. USA *101*, 4059–4064.

Frank, J., Zhu, J., Penczek, P., Li, Y., Srivastava, S., Verschoor, A., Radermacher, M., Grassucci, R., Lata, R.K., and Agrawal, R.K. (1995). A model of protein synthesis based on cryo-electron microscopy of the *E. coli* ribosome. Nature *376*, 441–444.

Fulle, S., and Gohlke, H. (2009). Statics of the ribosomal exit tunnel: implications for cotranslational peptide folding, elongation regulation, and antibiotics binding. J. Mol. Biol. *387*, 502–517.

Gong, F., and Yanofsky, C. (2002). Instruction of translating ribosome by nascent peptide. Science *297*, 1864–1867.

Graham, M.Y., and Weisblum, B. (1979). 23S ribosomal ribonucleic acid of macrolide-producing streptomycetes contains methylated adenine. J. Bacteriol. *137*, 1464–1467.

Hamilton-Miller, J.M., and Shah, S. (1998). Comparative in-vitro activity of ketolide HMR 3647 and four macrolides against gram-positive cocci of known erythromycin susceptibility status. J. Antimicrob. Chemother. *41*, 649–653.

Hardesty, B., Picking, W.D., and Odom, O.W. (1990). The extension of polyphenylalanine and polylysine peptides on *Escherichia coli* ribosomes. Biochim. Biophys. Acta *1050*, 197–202.

Hartz, D., McPheeters, D.S., Traut, R., and Gold, L. (1988). Extension inhibition analysis of translation initiation complexes. Methods Enzymol. *164*, 419–425.

Hillebrecht, J.R., and Chong, S. (2008). A comparative study of protein synthesis in *in vitro* systems: from the prokaryotic reconstituted to the eukaryotic extract-based. BMC Biotechnol. *8*, 58.

Hilliard, J.J., Goldschmidt, R.M., Licata, L., Baum, E.Z., and Bush, K. (1999). Multiple mechanisms of action for inhibitors of histidine protein kinases from bacterial two-component systems. Antimicrob. Agents Chemother. *43*, 1693–1699.

Horinouchi, S., and Weisblum, B. (1980). Posttranscriptional modification of mRNA conformation: mechanism that regulates erythromycin-induced resistance. Proc. Natl. Acad. Sci. USA *77*, 7079–7083.

Huber, D., Rajagopalan, N., Preissler, S., Rocco, M.A., Merz, F., Kramer, G., and Bukau, B. (2011). SecA interacts with ribosomes in order to facilitate posttranslational translocation in bacteria. Mol. Cell *41*, 343–353.

Ito, K., Chiba, S., and Pogliano, K. (2010). Divergent stalling sequences sense and control cellular physiology. Biochem. Biophys. Res. Commun. *393*, 1–5.

Kanehisa, M., Goto, S., Kawashima, S., and Nakaya, A. (2002). The KEGG databases at GenomeNet. Nucleic Acids Res. *30*, 42–46.

Kohanski, M.A., Dwyer, D.J., Hayete, B., Lawrence, C.A., and Collins, J.J. (2007). A common mechanism of cellular death induced by bactericidal antibiotics. Cell *130*, 797–810.

Lovmar, M., Nilsson, K., Vimberg, V., Tenson, T., Nervall, M., and Ehrenberg, M. (2006). The molecular mechanism of peptide-mediated erythromycin resistance. J. Biol. Chem. *281*, 6742–6750.

Lovmar, M., Nilsson, K., Lukk, E., Vimberg, V., Tenson, T., and Ehrenberg, M. (2009). Erythromycin resistance by L4/L22 mutations and resistance masking by drug efflux pump deficiency. EMBO J. *28*, 736–744.

Mankin, A.S. (2008). Macrolide myths. Curr. Opin. Microbiol. *11*, 414–421.

Mayford, M., and Weisblum, B. (1989). *ermC* leader peptide. Amino acid sequence critical for induction by translational attenuation. J. Mol. Biol. *206*, 69–79.

Menninger, J.R. (1995). Mechanism of inhibition of protein synthesis by macrolide and lincosamide antibiotics. J. Basic Clin. Physiol. Pharmacol. *6*, 229–250.

Menninger, J.R., Coleman, R.A., and Tsai, L.N. (1994). Erythromycin, lincosamides, peptidyl-tRNA dissociation, and ribosome editing. Mol. Gen. Genet. *243*, 225–233.

Moazed, D., and Noller, H.F. (1987). Chloramphenicol, erythromycin, carbomycin and vernamycin B protect overlapping sites in the peptidyl transferase region of 23S ribosomal RNA. Biochimie *69*, 879–884.

Moore, S.D., and Sauer, R.T. (2008). Revisiting the mechanism of macrolide-antibiotic resistance mediated by ribosomal protein L22. Proc. Natl. Acad. Sci. USA *105*, 18261–18266.

Nakatogawa, H., and Ito, K. (2002). The ribosomal exit tunnel functions as a discriminating gate. Cell *108*, 629–636.

Nissen, P., Hansen, J., Ban, N., Moore, P.B., and Steitz, T.A. (2000). The structural basis of ribosome activity in peptide bond synthesis. Science *289*, 920–930.

O'Farrell, P.H. (1975). High resolution two-dimensional electrophoresis of proteins. J. Biol. Chem. *250*, 4007–4021.

Odom, O.W., Picking, W.D., Tsalkova, T., and Hardesty, B. (1991). The synthesis of polyphenylalanine on ribosomes to which erythromycin is bound. Eur. J. Biochem. *198*, 713–722.

Oleinick, N.L. (1975). The Erythromycins. In Antibiotics, Vol. 3, Mechanism of action of antimicrobial and tumor agents, J.W. Corcoran and F.E. Hahn, eds. (New York: Springer-Verlag), pp. 397–419.

Onouchi, H., Nagami, Y., Haraguchi, Y., Nakamoto, M., Nishimura, Y., Sakurai, R., Nagao, N., Kawasaki, D., Kadokura, Y., and Naito, S. (2005). Nascent peptide-mediated translation elongation arrest coupled with mRNA degradation in the CGS1 gene of *Arabidopsis*. Genes Dev. *19*, 1799–1810.

Otaka, T., and Kaji, A. (1975). Release of (oligo) peptidyl-tRNA from ribosomes by erythromycin A. Proc. Natl. Acad. Sci. USA *72*, 2649–2652.

Peltz, S.W., Welch, E.M., Trotta, C.R., Davis, T., and Jacobson, A. (2009). Targeting post-transcriptional control for drug discovery. RNA Biol. *6*, 329–334.

Pestka, S. (1972). Studies on transfer ribonucleic acid-ribosome complexes. XIX. Effect of antibiotics on peptidyl puromycin synthesis on polyribosoms from *Escherichia coli*. J. Biol. Chem. *247*, 4669–4678.

Ramu, H., Mankin, A., and Vázquez-Laslop, N. (2009). Programmed drug-dependent ribosome stalling. Mol. Microbiol. *71*, 811–824.

Ramu, H., Vázquez-Laslop, N., Klepacki, D., Dai, Q., Piccirilli, J., Micura, R., and Mankin, A.S. (2011). Nascent peptide in the ribosome exit tunnel affects functional properties of the A-site of the peptidyl transferase center. Mol. Cell *41*, 321–330.

Schägger, H., and von Jagow, G. (1987). Tricine-sodium dodecyl sulfate-polyacrylamide gel electrophoresis for the separation of proteins in the range from 1 to 100 kDa. Anal. Biochem. *166*, 368–379.

Schlünzen, F., Zarivach, R., Harms, J., Bashan, A., Tocilj, A., Albrecht, R., Yonath, A., and Franceschi, F. (2001). Structural basis for the interaction of antibiotics with the peptidyl transferase centre in eubacteria. Nature *413*, 814–821.

Schmeing, T.M., Huang, K.S., Strobel, S.A., and Steitz, T.A. (2005). An induced-fit mechanism to promote peptide bond formation and exclude hydrolysis of peptidyl-tRNA. Nature *438*, 520–524.

Seidelt, B., Innis, C.A., Wilson, D.N., Gartmann, M., Armache, J.P., Villa, E., Trabuco, L.G., Becker, T., Mielke, T., Schulten, K., et al. (2009). Structural insight into nascent polypeptide chain-mediated translational stalling. Science *326*, 1412–1415.

Shimizu, Y., Kanamori, T., and Ueda, T. (2005). Protein synthesis by pure translation systems. Methods *36*, 299–304.

Starosta, A.L., Karpenko, V.V., Shishkina, A.V., Mikolajka, A., Sumbatyan, N.V., Schluenzen, F., Korshunova, G.A., Bogdanov, A.A., and Wilson, D.N. (2010). Interplay between the ribosomal tunnel, nascent chain, and macrolides influences drug inhibition. Chem. Biol. *17*, 504–514.

Tai, P.C., Wallace, B.J., and Davis, B.D. (1974). Selective action of erythromycin on initiating ribosomes. Biochemistry *13*, 4653–4659.

Taubman, S.B., So, A.G., Young, F.E., Davie, E.W., and Corcoran, J.W. (1963). Effect of erythromycin on protein biosynthesis in *Bacillus subtilis*. Antimicrob Agents Chemother (Bethesda) *161*, 395–401.

Tenson, T., and Mankin, A.S. (2001). Short peptides conferring resistance to macrolide antibiotics. Peptides *22*, 1661–1668.

Tenson, T., DeBlasio, A., and Mankin, A. (1996). A functional peptide encoded in the *Escherichia coli* 23S rRNA. Proc. Natl. Acad. Sci. USA *93*, 5641–5646.

Tenson, T., Xiong, L., Kloss, P., and Mankin, A.S. (1997). Erythromycin resistance peptides selected from random peptide libraries. J. Biol. Chem. *272*, 17425–17430.

Tenson, T., Lovmar, M., and Ehrenberg, M. (2003). The mechanism of action of macrolides, lincosamides and streptogramin B reveals the nascent peptide exit path in the ribosome. J. Mol. Biol. *330*, 1005–1014.

Tu, D., Blaha, G., Moore, P.B., and Steitz, T.A. (2005). Structures of MLS_BK antibiotics bound to mutated large ribosomal subunits provide a structural explanation for resistance. Cell *121*, 257–270.

Vázquez, D. (1966). Antibiotics affecting chloramphenicol uptake by bacteria. Their effect on amino acid incorporation in a cell-free system. Biochim. Biophys. Acta *114*, 289–295.

Vázquez, D. (1979). Inhibitors of protein biosynthesis (Berlin, Heidelberg, New York: Springer-Verlag).

Vázquez-Laslop, N., Thum, C., and Mankin, A.S. (2008). Molecular mechanism of drug-dependent ribosome stalling. Mol. Cell *30*, 190–202.

Vázquez-Laslop, N., Ramu, H., Klepacki, D., Kannan, K., and Mankin, A.S. (2010). The key function of a conserved and modified rRNA residue in the ribosomal response to the nascent peptide. EMBO J. *29*, 3108–3117.

Vázquez-Laslop, N., Ramu, H., and Mankin, A.S. (2011a). Nascent peptide–mediated ribosome stalling promoted by antibiotics. In Ribosomes: Structure, Function, and Dynamics, M.V. Rodnina, R. Green, and W. Wintermeyer, eds. (Vienna: Springer-Verlag), pp. 377–392.

Vázquez-Laslop, N., Klepacki, D., Mulhearn, D.C., Ramu, H., Krasnykh, O., Franzblau, S., and Mankin, A.S. (2011b). Role of antibiotic ligand in nascent peptide-dependent ribosome stalling. Proc. Natl. Acad. Sci. USA *108*, 10496–10501.

Voss, N.R., Gerstein, M., Steitz, T.A., and Moore, P.B. (2006). The geometry of the ribosomal polypeptide exit tunnel. J. Mol. Biol. *360*, 893–906.

Weisblum, B. (1995). Insights into erythromycin action from studies of its activity as inducer of resistance. Antimicrob. Agents Chemother. *39*, 797–805.

Woosley, L.N., Castanheira, M., and Jones, R.N. (2010). CEM-101 activity against Gram-positive organisms. Antimicrob. Agents Chemother. *54*, 2182–2187.

Yao, S., Blaustein, J.B., and Bechhofer, D.H. (2008). Erythromycin-induced ribosome stalling and RNase J1-mediated mRNA processing in *Bacillus subtilis*. Mol. Microbiol. *69*, 1439–1449.

Yonath, A., Leonard, K.R., and Wittmann, H.G. (1987). A tunnel in the large ribosomal subunit revealed by three-dimensional image reconstruction. Science *236*, 813–816.

Zaporojets, D., French, S., and Squires, C.L. (2003). Products transcribed from rearranged *rrn* genes of *Escherichia coli* can assemble to form functional ribosomes. J. Bacteriol. *185*, 6921–6927.

Zhanel, G.G., and Hoban, D.J. (2002). Ketolides in the treatment of respiratory infections. Expert Opin. Pharmacother. *3*, 277–297.